



# Countermanding saccades with auditory stop signals: testing the race model

Hans Colonius \*, Jale Özyurt, Petra A. Arndt

*Institut für Kognitionsforschung, Universität Oldenburg, FB5-A6, D-26111 Oldenburg, Germany*

Received 14 August 2000; received in revised form 19 February 2001

## Abstract

In a stop signal paradigm to investigate the control of human saccades subjects were instructed to make a saccade to a visual target appearing suddenly 15° to the left or to the right of the fixation point. In 25% of the trials an auditory stop signal was presented after a variable delay that required the subject to inhibit the saccade. The stop signal was presented randomly at the target position, at the opposite side, or at fixation. Using different estimation techniques the average time needed to inhibit a saccade (stop signal processing time, or SSPT) was estimated on the basis of the race model. The SSPT estimates ranging from 50 to 100 ms (depending on subject) are shorter than those from previous studies with visual stop signals. Position of the auditory stop signal did not show an effect on countermanding effectiveness. We found saccadic response times consistent with the race model predictions for two subjects, while a third subject showed small but consistent violations. Moreover, all subjects showed a tendency towards hypometric saccades for responses that could not be inhibited. These findings are discussed with respect to recent neurophysiological results. © 2001 Elsevier Science Ltd. All rights reserved.

*Keywords:* Reaction time; Countermanding; Eye movement; Race model

## 1. Introduction

The control of action is an important part of an individual's capacity to quickly adapt to ongoing changes in the environment. It includes not only the ability to initiate and to maintain movements, but also to withhold a planned movement, or to stop or change a current action. The stop signal paradigm provides an excellent framework to study these fundamental adaptive achievements in a laboratory situation. In the simple stop signal task subjects are instructed to react as quickly as possible to target stimuli (go task) but to stop their reaction whenever a stop signal occurs with one of several delays after the presentation of the target (stop task). Commonly, stop trials occur in about 10–25% of all trials in a random order unpredictable to the subject. Inhibitory success in such a task depends on the time interval between the presentation of the go and the stop stimulus, on stimulus properties of both types of signals, as well as on possible subject strategies.

Typically, the later the stop signal occurs the smaller is the probability that the subject is able to stop the response.

Until recently, stop signal behavior has been studied with simple manual responses, hand squeezes, typewriting, and arm movements (see Logan (1994) for a review). In a series of studies by Carpenter, Hanes, Schall, and coworkers the stop signal paradigm has also been applied to investigate the control of oculomotor behavior in both humans and the macaque (Hanes & Schall, 1995, 1996; Hanes, Patterson, & Schall, 1998; Hanes & Carpenter, 1999). The task in these experiments was to suppress a saccadic response toward a visual target as soon as a visual stop signal (reappearance of the fixation point) occurred. The study of saccadic eye movements by the stop signal paradigm seems particularly promising for unraveling the mechanisms underlying inhibitory control since orienting saccades are highly automated and their physiological mechanisms have been studied in depth (e.g. Leigh & Zee, 1999).

The purpose of this paper is to enhance the study of stop signal behavior in an eye movement control task

\* Corresponding author. Tel./fax: +49-441-7985158.

E-mail address: hans.colonius@uni-oldenburg.de (H. Colonius).

by using an auditory, rather than a visual stop signal. Previous studies with other control tasks suggest that countermanding is an amodal, central process that can be activated in different ways (c.f. Logan, 1994). Is this also true for the inhibition of an eye movement? Moreover, we were interested in whether varying the spatial position of the stop signal relative to the go signal affects performance. Obviously, a stop signal in close proximity to the target stimulus could be more effective, less effective, or have the same effect compared to a more distant stop signal. In any event, the result could be informative with respect to the functional organization of the underlying neural processes. In particular, it has been suggested by Schall and Thompson (1999) that the effectiveness of a visual stop signal presented foveally is due to its direct activation of the gaze fixation system. However, a recent study by Asrress and Carpenter (2001) showed no significant differences between central and peripheral visual stop signals. This issue will be taken up again in the final section where some additional results will be discussed.

The second purpose of this paper is to probe the race model proposed by Logan and Cowan (1984) and its specific version proposed in Hanes and Carpenter (1999) for the eye movement countermanding task. The structure of this paper is as follows. First, the race model for the stop signal paradigm by Logan and Cowan is described and some predictions of the race model are derived that — it seems — have not been considered in the literature yet. Second, an experiment is reported that studies the effect of presenting an auditory stop signal to cancel a saccadic response to a visual go-signal. Dependent variables were saccadic response time, amplitude, and peak velocity of the eye movements as well as the probability to cancel a movement when a stop signal is presented. Finally, the data will be used as a test of both the general and the specific race model.

## 2. The race model

Observable performance in the stop signal paradigm clearly exhibits stochastic variability. In any given trial with a stop signal present, it is not predictable with certainty whether or not a response will be inhibited. Moreover, features of the hand or eye movement (saccadic reaction time, amplitude, velocity) typically vary from trial to trial. Therefore, a stochastic mechanism has been postulated to underlie performance in this type of task very early on (e.g. Lappin & Eriksen, 1966; Ollman, 1973). It is assumed to consist of at least two parts, a GO process and a STOP process that race against each other. The response to the go signal is inhibited whenever the STOP process finishes before the

GO process. In the oculomotor task, the GO process includes programming the metrics of the saccade and its initiation, whereas the STOP process seeks to inhibit movement initiation. A reader mainly interested in the experimental results should skip the rest of this section and go on to Section 3.

### 2.1. The Logan–Cowan model: assumptions and predictions

Logan and Cowan (1984) analyzed the race model in terms of the finishing times of the STOP and the GO process and developed methods to estimate the non-observable duration of the STOP process and to account for the observable distributions of reaction times in go and in stop trials. Let  $T_{GO}$  and  $T_{STOP}$  denote the random finishing times of the GO and the STOP process, respectively, and let  $t_d$  stand for the stop signal delay (SSD), i.e. the time between the onset of the go signal and the onset of the stop signal. According to the race model, the probability to inhibit the response then equals:

$$P[T_{GO} > T_{STOP} + t_d] = q(t_d), \quad (1)$$

where  $q(t_d)$  is called the *inhibition function*. There are two empirically observable distribution functions, the distribution of go signal responses without a stop signal occurring (also called *control latency distribution*):

$$P[T_{GO} \leq t | \text{no stop signal presented}] = F_{GO}(t),$$

and the distribution of go signal responses given although a stop signal occurred (also called *stop failure response time distribution*):

$$P[T_{GO} \leq t | T_{GO} < T_{STOP} + t_d] = F_{GO}(t; t_d), \quad (2)$$

with  $t \geq 0$  whereas neither the distribution for the stop signal processing time (SSPT)  $T_{STOP}$ :

$$P[T_{STOP} \leq t | t_d] = F_{STOP}(t; t_d),$$

nor the joint distribution for  $(T_{GO}, T_{STOP})$ :

$$P[T_{GO} \leq s \cap T_{STOP} \leq t | t_d],$$

with  $s, t \geq 0$  is observable (here,  $P[| t_d]$  refers to a conditional probability with conditioning on the event {stop signal presented  $t_d$  ms after onset of the go signal}). In order to yield an estimate of the unobservable STOP process distribution three assumptions have been added to the race model. The first, *context independence*, requires that the distribution of the GO process is the same whether or not a stop signal is present. The second, *stochastic independence*, stipulates that the finishing times of the GO process and the STOP process are stochastically independent. Note that, since the non-observable STOP process occurs in both assumptions, neither of these independence properties consid-

ered alone is falsifiable by behavioral data.<sup>1</sup> Third, it is assumed that the distribution of the STOP process does not depend on the time the stop signal is presented (*SSD invariance*).

Under these assumptions, the observed go signal response times and the inhibition function can be used both to estimate the mean of the unobservable *stop signal processing time*<sup>2</sup> (SSPT) ( $E[T_{STOP}]$ ), i.e. the time required to cancel the saccade being programmed, and to predict the distribution of response times in stop-task trials, i.e. the distribution of stop failure saccadic responses. Observing that the probability that a response occurs with stop signal delay  $t_d$ ,  $1 - q(t_d)$ , can formally be treated as a distribution function of some random variable  $T_d$ , Logan and Cowan (1984) showed that mean SSPT is equal to the difference between the mean reaction time in go trials and the mean of  $T_d$ :

$$E[T_{STOP}] = E[T_{GO}] - E[T_d], \quad (3)$$

leading to a simple estimation procedure for the unobservable mean stop signal processing time (see Section 3). Another method, proposed by Colonius (1990) (see also Logan (1994)), is based on the observation that:

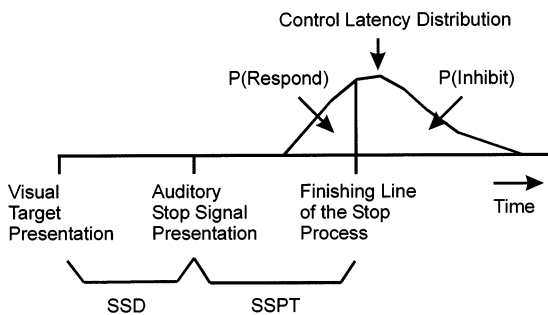


Fig. 1. Presentation of an auditory stop signal after a variable time delay with respect to the target stimulus initiates internal inhibitory processes. Stop signal processing is assumed to require a constant time (SSPT), adding to a given SSD. The finishing time of the stop process divides the control latency distribution into two parts. The left part of the distribution represents the probability of responding to the go signal  $P(\text{Respond})$ . These responses are fast enough to escape inhibition. The right part of the distribution represents the probability of inhibition given a stop signal  $P(\text{Inhibit})$ .

<sup>1</sup> Since the probabilities  $P[T_{GO} \leq t | \text{no stop signal presented}]$  and  $P[T_{GO} \leq t | T_{GO} < T_{STOP} + t_d]$  refer to two different experimental conditions, these independence assumptions are logically independent of each other. In fact, assume that stochastic independence between  $T_{GO}$  and  $T_{STOP}$  holds. It is nonetheless possible, e.g. due to some hypothetical limited capacity mechanism, that the mere presence of a stop signal goes along with slower processing of the GO signal, i.e.  $F_{GO}(t) \geq F_{GO}(t; t_d)$ . In the same vein, context independence may be satisfied, but  $T_{GO}$  and  $T_{STOP}$  may nonetheless be correlated.

<sup>2</sup> A more common term for this is stop signal response time (SSRT); the change in terminology is suggested here because stop signal processing time is not an observable response time but, rather, a hypothetical, unobservable concept of the race model.

$$P[T_{STOP} + t_d > t | t_d] = (1 - q(t_d))f_{GO}(t; t_d)/f_{GO}(t), \quad (4)$$

where  $f_{GO}(t; t_d)$  and  $f_{GO}(t)$  refer to the density function of observed response times with and without a stop signal, respectively. While this method has the advantage of estimating the entire distribution of stop signal processing times, it requires estimates of the density functions at a level of smoothness that cannot be obtained from typical empirical data (see Band (1997) for relevant simulation studies).

Another method of estimating mean SSPT (called the integration method) is based on the additional assumption, first proposed in Logan (1981), that stop signal processing time is constant. Although unlikely to be valid in a strict sense, simulation studies by De Jong, Coles, Logan, and Gratton (1990) and Band (1997) suggest that violations of this assumption have limited consequences, at least as far as estimation of mean SSPT is concerned. As illustrated in Fig. 1, SSPT then is the difference between the point at which the stop signal was presented ( $t_d$ ) and the point at which the stopping process finished ( $t_d + t_{STOP}$ ). The latter point can be estimated from the observed control latency distribution by integrating it until the area under the integral equals the probability of responding. Performing this procedure for each stop signal delay and averaging the values often yields a stable estimate for the mean stop signal processing time.

This illustration suggests a method to predict mean reaction time in stop trials by averaging over response times occurring to the left of the finishing time of the STOP process. Typically, satisfactory predictions can only be obtained for large SSDs where stop failure responses are more numerous than for small SSDs.

Interestingly, the *complete race model*, i.e. without assuming constant stop signal processing time, predicts an upper and a lower bound for the (observable) distribution of stop failure responses. Since this result, to our knowledge, has not been reported in the literature yet, it is given in the following proposition (for a proof, see Appendix A).

**Proposition 1.** *Assuming the complete race model holds, i.e. there is (i) stochastic independence between  $T_{GO}$  and  $T_{STOP}$  with  $F_{GO}(0) = F_{STOP}(t_d) = 0$  and (ii) context independence holds, i.e.  $P[T_{GO} \leq t | \text{no stop signal presented}] = P[T_{GO} \leq t \cap T_{STOP} \leq \infty | t_d]$  and, moreover,  $P[T_{GO} < T_{STOP} + t_d] > 0$  for any SSD  $t_d(t_d > 0)$ , then:*

$$\begin{aligned} F_{GO}(t) &= P[T_{GO} \leq t | \text{no stop signal presented}] \\ &\leq P[T_{GO} \leq t | T_{GO} < T_{STOP} + t_d] = F_{GO}(t; t_d) \\ &\leq F_{GO}(t)/P[T_{GO} < T_{STOP} + t_d] \end{aligned} \quad (5)$$

for all  $t, t \leq 0$ .

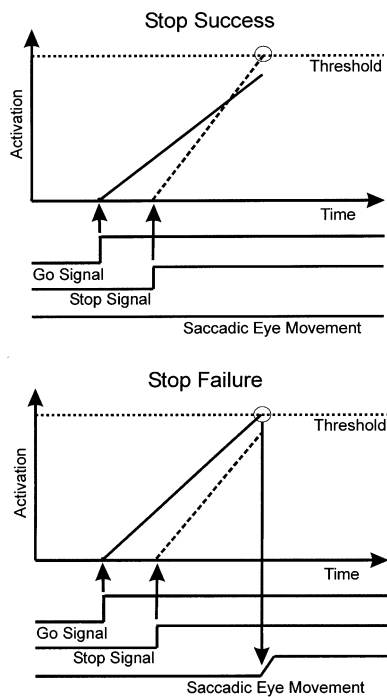


Fig. 2. Basic assumptions of the Hanes–Carpenter model. In stop trials presentation of a visual target stimulus and delayed presentation of an auditory stop signal initiates internal response (solid line) and inhibitory processes (dashed line), respectively. In an independent race both processes rise linearly toward a threshold. If the inhibitory process overtakes the go process and reaches the threshold first, the response to the target is withheld successfully (upper panel). Otherwise, if the go process wins the race, inhibition fails and a response to the target occurs (lower panel).

Thus, in the race model the distribution of stop failure reaction times has the distribution of go signal reaction times as a lower bound, and dividing the latter distribution by the probability of responding in the presence of a stop signal yields an upper bound as well. In particular, the lower bound implies a corresponding inequality for the means:

$$E[T_{GO} | T_{GO} < T_{STOP} + t_d] \leq E[T_{GO}]. \quad (6)$$

Thus, this last prediction, i.e. that mean stop failure responses should be faster than mean go signal responses, does hold in general, not only with a constant stop signal processing time.

## 2.2. The Hanes–Carpenter model

Carpenter, Hanes, Schall, and coworkers proposed a specific version of the Logan–Cowan race model and tested it on a stop signal task both with human subjects (Hanes & Carpenter, 1999) and monkeys (Hanes & Schall, 1995; Hanes et al., 1998). It is based on the LATER model (linear approach to threshold with ergodic rate) by Carpenter (Carpenter, 1981; Carpenter & Williams, 1995) which assumes that the response prepa-

ration signal initiated by the target rises in a linear fashion to a fixed activity threshold, with the rate of rise varying randomly from trial to trial. For the stop signal task it is additionally assumed that both the go signal and the stop signal initiate a linear rise to a threshold value. If the stop process reaches the threshold before the go signal process, movement is inhibited. Otherwise the saccade is executed (stop signal failure). Assuming normally distributed rates of rise (Hanes & Carpenter, 1999) with possibly different means and standard deviations, this model obviously constitutes a specific instance of the Logan–Cowan model (Fig. 2).

Note that the rates are assumed to be normally distributed, but the distribution functions for the go signal and the stop signal processing times for this model have a skewed distribution (see Appendix B for an explicit expression of the density functions).

## 3. Experiment

In the experiment reported here an auditory noise at different spatial positions was used as stop signal to inhibit a saccadic response toward a visual target stimulus. Besides testing whether this change of modality implies an improvement in stop signal performance compared to earlier studies, we were especially interested in whether varying the spatial position of the stop signal relative to the go signal affects stopping performance. The experiment also served as a further test of the race model both in its general version and in the Hanes–Carpenter special case. The results of the model tests will be presented in Section 4.

### 3.1. Method

#### 3.1.1. Participants

Three subjects (MR, male, age 40; DL, female, 23; NL, female, 21) with normal hearing abilities, and normal or corrected-to-normal visual acuity were tested. All subjects had right eye dominance. The experiment was carried out with the understanding and consent of each subject.

#### 3.1.2. Apparatus and stimuli

Subjects were seated in a darkened, sound attenuated chamber (1.0 × 1.2 × 1.9 m). The head was held steady by a dental impression plate. Visual stimuli were presented on a 37 in. monitor (XP37, NEC) at a distance of 57 cm. The monitor update rate was 75 Hz. Auditory stimuli (noise signal of bandwidth 500–14000 Hz) were presented via a virtual acoustic environment through headphones (Sennheiser HD 580). The noise signal was convolved with head related transfer functions of a dummy head to generate the three auditory positions

used in the experiment. They were presented with an intensity of 72 dB SPL via headphones. The rise time of the noise signal was 5 ms. White dots with a diameter of 0.10 served as visual targets and fixation point (19.8 cd/m<sup>2</sup>) and were presented on a dark background (less than 0.01 cd/m<sup>2</sup>). The presentation of both stimuli was controlled by a PC, a second PC was employed for data acquisition. The temporal arrangement of stimulus presentation and data acquisition were synchronized with the exact presentation time of the visual stimulus determined by the monitor update rate.

### 3.1.3. Design

All stimuli were presented on the horizontal plane. Visual stimuli were presented at two different positions (left:  $-15^\circ$ , right:  $+15^\circ$ ) whereas auditory stimuli were presented via virtual acoustics at three different positions ( $0^\circ$  (i.e. in front of the subject),  $+15^\circ$ ,  $-15^\circ$ ). The stop signal delay was varied on five levels with equal probability. Combination of two visual stimuli  $\times$  three auditory stimuli  $\times$  five stop-signal delays resulted in 30 stop conditions. These stop trials were randomly interspersed with control trials in each experimental block consisting of 120 trials altogether.

### 3.1.4. Task

Subjects were instructed to fixate properly and to make a saccade in the direction of the visual stimulus as quickly as possible. They were instructed to inhibit their reaction toward the target if an auditory signal was presented.

### 3.1.5. Response recording and detection

Eye movements were measured with an infrared light reflecting system (IRIS, Skalar Medicals) in training and experimental sessions. This system provides an analog signal of the eye position that was digitized at a rate of 1 kHz and stored for further analysis. Spatial resolution after calibration and digitization was maximally  $0.2^\circ$ . Saccade onsets and offsets were identified automatically, using velocity criteria ( $50^\circ/\text{s}$  for onsets and  $20^\circ/\text{s}$  for offsets). The accuracy of the computer generated marks was verified by inspection of the records displayed on a graphics monitor. Trials including blinks, small saccades or drifts larger than  $0.8^\circ$  during fixation, anticipations (latencies less than 80 ms) or other errors were excluded from further analysis. Saccades larger than  $1^\circ$  into the direction of the target carried out during the first 500 ms after target presentation were considered as responses. Saccadic reaction time was determined as time difference between target onset and saccade onset. For the analysis of saccadic amplitudes only data from measurements with good and stable calibration were used.

### 3.1.6. Experimental procedure

Each trial started with the onset of a fixation point, presented for a random time interval (minimum 1300 ms). The visual target (go signal) was presented for 500 ms after a variable foreperiod, 800 ms after the onset of the fixation point at the earliest. In 25% of the experimental trials an auditory stop signal was presented for 500 ms with one stop signal delay out of five possible delays with respect to the visual stimulus. If reaction time exceeded an individually determined criterion, the subject received feedback 2 s after the onset of the visual target. A red dot presented for 200 ms at the position of the fixation point served as feedback stimulus ( $0.1^\circ$ , 6.4 cd/m<sup>2</sup>). The intertrial time was 1.5 s, starting with the offset of the feedback stimulus or, in trials without feedback, 2 s after the onset of the visual target. At the end of each experimental block subjects received feedback about their mean reaction time and the proportion of successfully inhibited reactions in stop signal trials.

### 3.1.7. Training

Subjects took part in 11 training sessions until their performance stabilized. The last three to four sessions served to determine an individual reaction time criterion and to fix individual stop signal delays. The reaction time criterion  $C$  was chosen to be exceeded by the slowest 20% of reaction times in control trials.<sup>3</sup>

Exceeding the reaction time criterion resulted in the presentation of a red dot to encourage the subjects to speed up their response to the go signal. This feedback was expected to minimize a speed–accuracy tradeoff as the most probable subject strategy. The individual delays were set to obtain probabilities of inhibition of approximately 0.85, 0.65, 0.5, 0.35, and 0.15.

## 3.2. Results

Excluding saccades associated with blinks and improper fixation, a total of 8203 (MR), 4507 (NL) and 3900 (DL) eye movements that were used for further analysis of reaction times and inhibition probabilities. For the analysis of saccadic amplitudes and peak velocities 7724 (MR), 3373 (NL), and 3896 (DL) eye movements additionally met the requirement of stable calibration. The dependent variables measured were saccadic latency, amplitude, and peak velocity in both the stop and the control condition as well as probability of response when a stop signal was given.

<sup>3</sup> For each session  $i$  the time value for  $C$  was computed utilizing mean reaction time  $RT$  and S.D.  $s$  of control trials in the previous session:  $C_i = RT_{i-1} + 9/10s_{i-1}$ .

3.2.1. Saccadic reaction times

Table 1 compares overall mean latencies in control versus stop failure trials for each subject. For two subjects (NL and DL) latencies are significantly reduced in stop failure trials ( $P < 0.001$ , 2-tailed Mann–Whitney  $U$ -test). For subject MR no significant difference between latencies in the two conditions was found.

Mean stop failure latencies increased with increasing stop signal delay for all subjects and stop signal delays (SSD), with the exception of the first SSD-condition of subject MR. The percentage of stop failure responses also increased with increasing stop signal delay (Table 2).

3.2.2. Saccadic amplitude

Saccadic amplitude differences between the stop failure and the control condition were found for subject MR for mean saccadic amplitudes both with rightward

Table 1  
Mean latency (RT) and S.E.M. for control and stop failure trials (in ms)

	MR	NL	DL
<i>Control condition</i>			
<i>N</i>	6123	3357	2919
<i>RT</i>	255	266	272
<i>S.E.M.</i>	0.4	0.7	0.9
<i>Stop failure condition</i>			
<i>N</i>	1018	622	511
<i>RT</i>	255	253	251
<i>S.E.M.</i>	1.2	1.4	1.7

Table 2  
Percentage and number of stop failure trials, mean latencies (RT) and S.E.M. for the five SSD of each subject (in ms)

	SSD1	SSD2	SSD3	SSD4	SSD5
<i>MR</i>					
<i>Delay</i>	90	120	150	180	210
<i>Stop failure (%)</i>	5.5	17.7	46.7	78.8	96.4
<i>N</i>	23	74	193	327	401
<i>RT</i>	287	243	248	256	258
<i>S.E.M.</i>	14.4	6.0	2.7	1.8	1.7
<i>NL</i>					
<i>Delay</i>	160	190	210	230	260
<i>Stop failure (%)</i>	12.0	34.3	57.4	77.3	90.8
<i>N</i>	28	80	132	174	208
<i>RT</i>	230	239	246	256	263
<i>S.E.M.</i>	8.6	4.1	2.9	2.7	2.3
<i>DL</i>					
<i>Delay</i>	150	200	230	250	270
<i>Stop failure (%)</i>	7.0	30.7	61.9	76.2	84.6
<i>N</i>	14	58	122	147	170
<i>RT</i>	188	227	249	251	265
<i>S.E.M.</i>	10.4	4.5	3.2	2.9	3.0

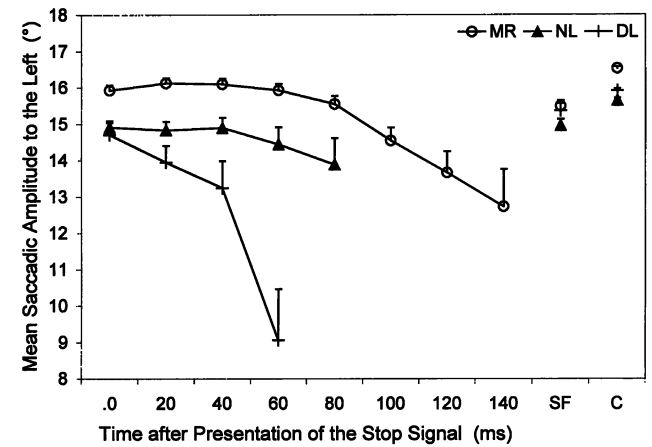
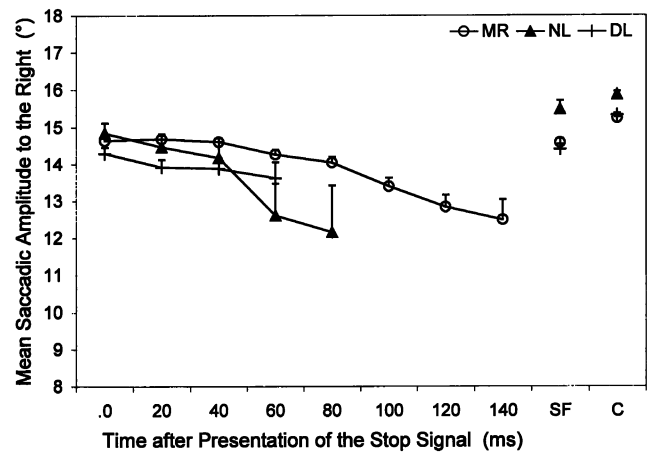


Fig. 3. Mean amplitudes of saccadic responses to the right (upper panel) and the left (lower panel) that occurred after the presentation of the stop signal. Each data point represents the mean amplitude of all responses that occurred from a given time point on after presentation of the stop signal (values on abscissa). ‘SF’ and ‘C’ denote mean amplitudes of all saccades in stop failure and control trials, respectively.

and leftward saccades ( $P < 0.001$ , Mann–Whitney  $U$ -test). Subject NL shows a significant difference for rightward saccades ( $P = 0.002$ ) and DL for leftward saccades ( $P < 0.001$ ) only. Given that a certain proportion of stop failure saccades occurs before the onset of the stop signal, only saccades performed after presentation of the stop signal are included in Fig. 3.

This plot reveals a decrease of mean saccade amplitude with increasing temporal distance to the stop signal. Note, however, that by construction the points in Fig. 3 are not independent of each other. For example, the amplitude average at 40 ms includes all saccades that were measured at 40 ms after the stop signal or later. Fig. 4 permits a closer look at the dynamics by presenting the average amplitudes and peak velocities separately for each time bin of 20 ms indicated on the horizontal axis.

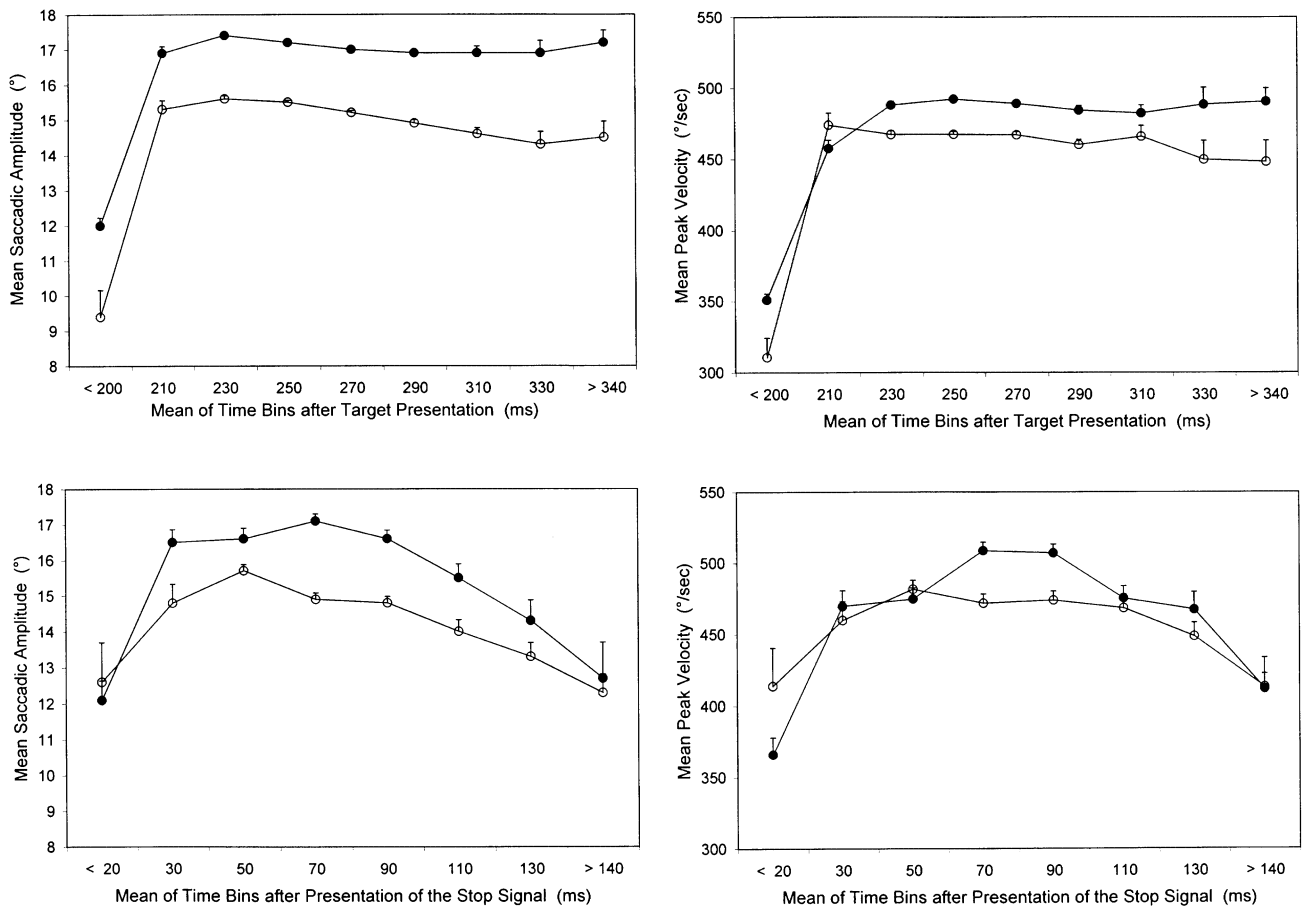


Fig. 4. Mean amplitudes (a) and mean peak velocities (b) of saccades in the control (upper panel) and the stop failure (lower panel) condition in different periods of time for subject MR. Periods of time are defined with respect to the presentation of the go stimulus and stop signal, respectively. Open circles denote amplitudes of saccadic movements to the right, whereas filled circles denote amplitudes of saccadic movements to the left.

For subject MR there is a clear tendency both in rightward and leftward eye movements toward hypometric saccades beginning 110 ms after presentation of the stop signal. Compared to the second time bin where performance is at the level of control trials, saccadic amplitudes are significantly reduced starting from 130 ms after stop signal presentation ( $P < 0.05$ , Mann–Whitney  $U$ -test). Moreover, only subject MR showed a reduction of saccadic amplitudes at a point in time when a stop signal presentation was likely to occur, i.e. during the first time bin. This reduction, presumably a result of an unconscious strategy by the subject, was significant both for control and stop failure trials and for both directions of eye movement ( $P < 0.05$ ).

For subject NL a significant reduction in mean saccadic amplitude can be observed beginning from 70 ms (rightward saccades) and for reactions occurring 80 ms after stop signal presentation and later (leftward saccades) ( $P < 0.05$ ). For subject DL mean size of eye movements in both directions is significantly reduced for saccades that were performed 60 ms after stop signal presentation and later ( $P < 0.05$ ).

### 3.2.3. Peak velocity

Comparing mean peak velocities of all saccades in the control and stop failure condition there is no significant reduction in stop failure trials. On the other hand, considering only those eye movements performed after a certain time delay after presentation of the stop signal, a decrease of mean peak velocities with increasing temporal distance to stop signal presentation can be found, similar to that for saccadic amplitudes, although not significant in all conditions. A significant reduction in mean saccadic peak velocity was obtained for subject MR for eye movements in both directions (Fig. 4b) and for subjects NL and DL for rightward and leftward saccades respectively ( $P < 0.05$ ).

### 3.2.4. Spatial effects

Varying spatial distance between auditory stop and visual go signals did not have any significant effect on mean saccadic RT and stopping performance, nor on saccadic amplitudes. Given this negative result, the data in the subsequent analyses have been aggregated over both visual and auditory positions (Fig. 5).

3.2.5. Inhibition functions

The probability to inhibit a response given a stop signal is presented at stop signal delay (SSD)  $t_d$  (c.f. Eq. (1)) is estimated by the relative frequency of successful inhibitions. These relative frequencies are plotted as a function of SSD separately for each subject in Fig. 6.

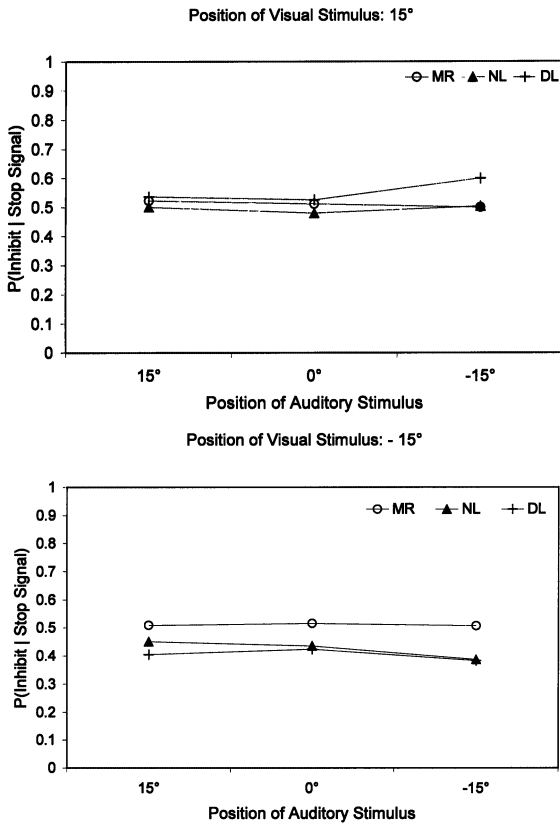


Fig. 5. Probability of inhibition for different spatial combinations of visual go and auditory stop signal. There is no significant effect of spatial stimulus arrangement.

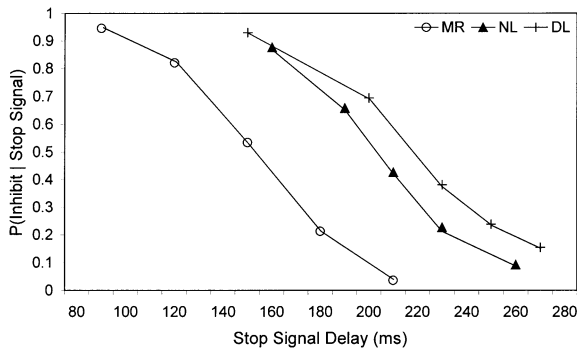


Fig. 6. Inhibition functions. For each subject the probability of saccadic inhibition in stop trials is plotted as a function of the stop signal delay. For a given stop-signal delay the probability to inhibit the response to the target is lower for subject MR than for subjects NL and DL.

According to the race model mechanism, delaying the onset of the stop signal decreases the probability of successful inhibition, since the chances of the STOP process to win the race will decrease with delaying its starting time. This monotonicity is obviously satisfied for our subjects.

3.3. Summary

While, obviously, saccadic latency always depends on stimulus parameters like target intensity and location, mean saccadic latencies for go-task trials measured for the three subjects in this experiment were within the range found in other recent studies using visual stop signals (Hanes & Carpenter, 1999; Logan & Irwin, 2000). For two of the subjects (NL, DL) mean latency was shorter (10–20 ms) for stop failures than for go responses. This decrease has also been observed in studies using visual, rather than auditory stop signals. Moreover, the inhibition functions are similar in shape for all subjects, the location differences merely reflecting differences in mean processing time both for the go and the stop signal among the subjects. The observation of hypometric saccades in stop failures responses is more surprising and has not yet been reported in the literature. Finally, the finding that the spatial position of the stop signal relative to the go signal did not affect inhibitory performance is of interest. In particular, auditory stop signals presented centrally were no more effective than stop signals presented at the periphery. Further interpretation and discussion of these experimental results is deferred until the general discussion in the final section.

4. Testing the Logan–Cowan race model

Predictions from the race model both in its most general form and from its more restrictive versions (specifically, assuming a constant STOP process) will be presented and discussed with respect to the data. Performance of the Hanes–Carpenter version will be dealt with in a separate subsection. For further details of the estimation procedures the reader is referred to Logan (1994).

4.1. Estimation of stop signal processing time (SSPT)

There are different methods to estimate the unobservable mean SSPT from the data (c.f. Section 2.1). We will compare estimates resulting from three different methods.

4.1.1. Integration method

Assuming the random variable  $T_{STOP}$  (SSPT) to be a constant ( $t_{STOP}$ ), its value can be estimated for each

Table 3  
Stop signal processing time (in ms) for all subjects and different methods of estimation<sup>a</sup>

	Integration	Mean	Median	Hanes–Carpenter
MR	103 ± 3.3	87	105	101
NL	60 ± 0.9	48	59	53
DL	51 ± 2.6	43	53	41

<sup>a</sup> S.E.M. is given where appropriate

stop signal delay by integrating over the latency distribution of the go signal until the integral equals the probability of responding for the given delay. Subtracting the stop signal delay from the upper bound of the integral then yields an estimate for  $t_{STOP}$ . Since the estimates varied very little for the different stop signal conditions, they were averaged over stop signal delays. They are presented ( $\pm$  S.E.M.) in the first column ('integration') of Table 3 for each of the subjects. Across all subjects the average ( $\pm$  S.E.M.) SSPT was  $71 \pm 16$  ms.

#### 4.1.2. Mean method

Here, SSPT is no longer assumed to be constant. The method is based on the idea that  $1 - q(t_d)$  ( $q(t_d)$ ) (the inhibition function) can formally be conceived of as a cumulative distribution corresponding to some random SSD variable  $T_d$ , say (c.f. Section 2.1). Mean SSPT can then be estimated from Eq. (3):

$$E[T_{STOP}] = E[T_{GO}] - E[T_d]$$

where  $E[T_d]$  is estimated as follows: Let  $P_i$  be the probability of responding at the  $i$ th stop signal delay  $SSD_i$  (Logan & Cowan, 1984):<sup>4</sup>

$$\text{Estimate of } E[T_d] = \sum_i [(P_i - P_{i-1})SSD_i].$$

The resulting estimates for the three subjects are presented in the second column ('Mean') of Table 3. Across all subjects the average ( $\pm$  S.E.M.) SSPT was  $59 \pm 14$  ms.

#### 4.1.3. Median method

Assuming a symmetric distribution for  $T_d$  it is possible to use the median to estimate its mean. The resulting estimates for the three subjects are presented in the third column ('Median') of Table 3. Across all subjects the average ( $\pm$  S.E.M.) SSPT was  $72 \pm 16$  ms.

The estimates resulting from the integration and the median method are in good agreement for each subject, whereas the mean method results in lower estimates. It

is possible that the mean method estimate suffers from the small number of observations for the small SSDs more than the median and the integration method.

#### 4.1.4. Predicted stop-failure latencies

Assuming constant SSPT, expected stop-failure latency for a given stop signal delay should equal the mean of the go latency distribution on the left part of the finishing line of the STOP process (see Fig. 1). Latencies of saccades in the stop signal condition were estimated for each stop signal delay and compared with empirically obtained latencies (Fig. 7). Note that we had enough observations even for the first SSD to include it in the analysis. Due to the small number of observations for the first stop signal delay, data from this condition are typically ignored. For the remaining SSDs there is a satisfactory agreement between estimated and observed mean stop-failure latencies for two of three subjects (NL and DL).

#### 4.2. Distribution inequality test for stop failure responses

Under the complete race model, i.e. when  $T_{STOP}$  is not assumed to be constant, the proposition in Section 2.1 provides a distribution-free test relating the observable cumulative distributions under the control and the stop failure conditions. Specifically, for any SSD the cumulative distribution of stop failures is bounded below by the cumulative distribution of the responses in the control condition. Moreover, the lower bound divided by the probability of a stop failure under the given SSD represents an upper bound for the distribution of the stop failures (c.f. Eq. (5)).

Considering the lower bound first, there were no significant violations for subjects DL and NL, whereas for subject MR violations for three of the five SSDs (SSD = 90, 180, and 210 ms) were found (Kolmogorov–Smirnov,  $P < 0.05$ , one-tailed) (Fig. 8).

For the upper bound, there were certain violations (c.f. the data from subject DL in Fig. 9), but none were statistically significant.<sup>5</sup>

#### 4.3. Discussion

First, using the established estimation techniques for the race model our analysis of the response times and the stopping frequencies has led to numerical estimates for the stop signal processing times (SSPT) of about 100, 60, and 50 ms for subjects MR, NL, and DL,

<sup>4</sup> If the observed inhibition function has a maximum less than 1, or a minimum greater than 0, this estimate must be rescaled by dividing by the difference between the maximum and the minimum probabilities of responding.

<sup>5</sup> Furthermore, as observed by Osman, Komblum, and Meyer (1986), the cumulative distributions for the stop failures should form a fan-shaped pattern in an order corresponding to increasing SSD values. This pattern is suggested by the data for subjects DL and NL, but it is not observed for subject MR (see Fig. 8).

respectively. Most notably, these estimates are 50–100 ms shorter than those from other recent studies with human saccades (Hanes & Carpenter, 1999; Logan & Irwin, 2000). Since our estimates were consistent over different estimation techniques (especially, for the integration and the median method), there seems to be no reason to doubt their validity, at least under the general hypothesis of the race model. Since the main difference of this study compared to those with longer SSPTs is our use of an auditory rather than a visual stop signal, it seems plausible to attribute this decrease to an effect

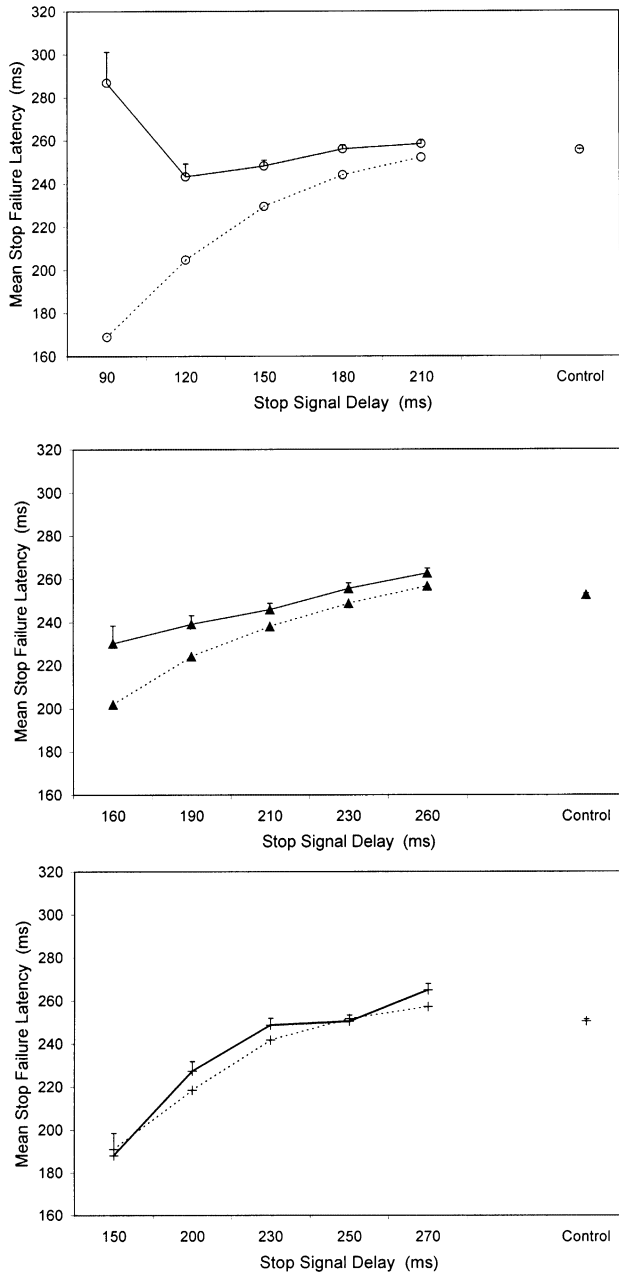


Fig. 7. Estimated (dashed line) and observed (solid line) stop failure latencies for the different stop signal delays for subjects MR (upper panel), NL (middle panel), and DL (lower panel).

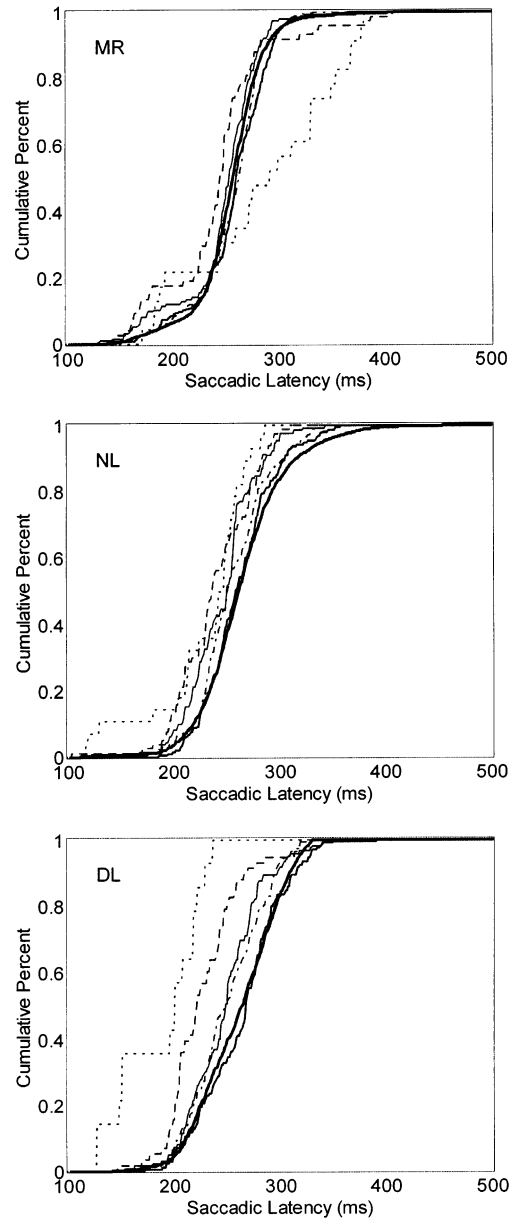


Fig. 8. Test of the lower boundary (Eq. (5)). Cumulative distribution functions of reaction times in SSD conditions should not cross the lower bound represented by the cumulative distribution function of reaction times in the control condition (thick line, control condition; dotted line, SSD1; dashes, SSD2; thin line, SSD3; dots/dashes, SSD4; medium line, SSD5).

of modality. This is in line with the faster peripheral processing and conduction time of auditory stimuli compared to visual stimuli.<sup>6</sup> However, a recent study by Cabel, Armstrong, Reingold, and Munoz (2000) found

<sup>6</sup> An auditory stimulus presented close to the ear takes approximately 13 ms to activate a superior colliculus neuron, a nearby visual stimulus requires about 65–100 ms to reach the same neurons (c.f. Stein & Meredith, 1993).

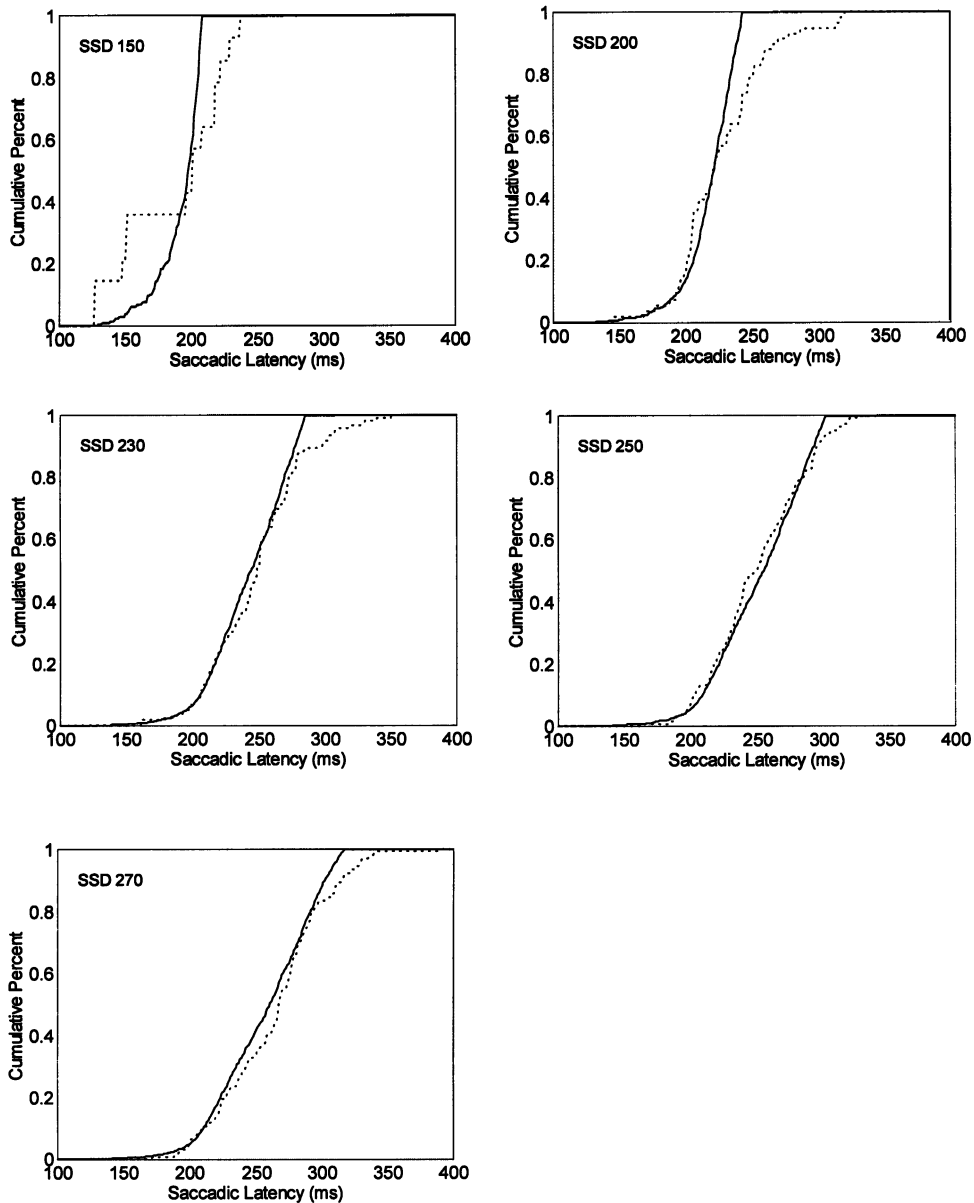


Fig. 9. Test of the upper boundary (Eq. (5)). Cumulative distribution functions for the different SSDs of subject DL.

longer SSPTs for auditory than for visual stop signals. How their results can be reconciled with our findings will be discussed in Section 6.

Second, we applied the distribution inequality test (c.f. the proposition above) to examine the validity of the complete race model. Such a test is valuable because, as pointed out in Section 2.1, the assumptions of the race model (i.e. context independence, stochastic independence of the finishing times of the STOP and the GO process, and stop signal delay invariance) cannot be tested separately. Moreover, Band (1997) has demonstrated in his extensive simulation studies that satisfactory agreement between observed and predicted stop failure latencies (c.f. Fig. 7) is not sufficient as a test of the independence assumptions (Band, *ibid.*, p.

141). Our test results clearly corroborate the race model for two of the subjects (DL and NL). For subject MR the inequality was violated for three of the five stop signal delays.

### 5. Testing the Hanes–Carpenter race model

As a specific version of the Logan–Cowan race model the Hanes–Carpenter model (c.f. Section 2.2) makes specific parametric predictions for the inhibition functions and the response time distributions in the control and the stop failure conditions. The model was tested on our data set using two different methods of parameter estimation. The first makes use of Monte

Carlo simulations as in the study by Hanes and Carpenter (1999) with visual go and stop signals. The second method is based on the explicit expressions for the distribution functions presented in Appendix B. The four parameters to be estimated are the means and standard deviations of the normally distributed rates of rise of the GO process and the STOP process, respectively,  $\mu_{GO}$ ,  $\sigma_{GO}$ ,  $\mu_{STOP}$ , and  $\sigma_{STOP}$ .

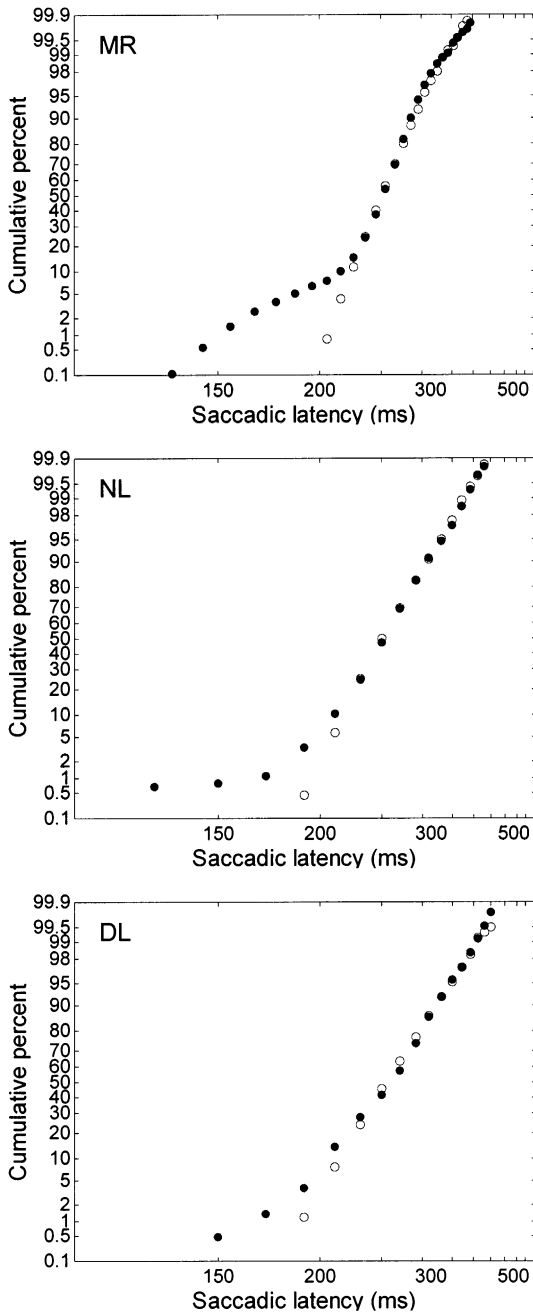


Fig. 10. Cumulative empirical latency distributions (filled symbols) and simulated distributions (open symbols) of the control condition, shown as reciprobital plots (i.e. with a reciprocal time axis and probit ordinate). Parameters  $\mu_{GO}$  and  $\sigma_{GO}$  are derived from these fits.

### 5.1. Estimation by Monte Carlo simulations

Here we followed the procedure described in Hanes and Carpenter (1999) as closely as possible (see *ibid.* for further details). The parameters were estimated separately for each subject in two steps. In the first step,  $\mu_{GO}$  and  $\sigma_{GO}$  were estimated from the actual distribution of the reaction times in the control condition. For each of the 2048 trials the rate of rise value  $r_{GO}$  was selected randomly from a normal distribution with parameters  $\mu_{GO}$  and  $\sigma_{GO}$ . Following Hanes and Carpenter (1999) we assumed an irreducible minimum processing time  $\tau_{visual}$  of 60 ms for the processing of the visual go signal. The value  $x_{GO}$  representing the decision signal was incremented at each time step (iteration). Iterations were performed in 1 ms steps. The point in time at which  $x_{GO}$  reached a threshold  $\theta$  (set equal to one) determined the response time for this trial. The values of  $\mu_{GO}$  and  $\sigma_{GO}$  were chosen to minimize the deviation between cumulative distribution function of the observed and the simulated data. Simulated and experimentally obtained distributions are shown in Fig. 10. They were not significantly different for any of the subjects ( $P > 0.1$ , 2-tailed Kolmogorov–Smirnov).<sup>7</sup>

In a second set of simulations estimates for  $\mu_{STOP}$  and  $\sigma_{STOP}$  were derived from the inhibition functions following the procedure in Hanes and Carpenter (1999). The GO process was simulated as before. Additionally the STOP process started  $t_d$  milliseconds after the onset of the trial. We chose  $\tau_{auditory} = 20$  ms as irreducible minimal processing time for the auditory stop signal. At each time step after  $t_d + 20$  ms the decision signal  $x_{STOP}$  of the STOP process was incremented by the value of  $r_{STOP}$  randomly chosen from the Gaussian distribution of rates of rise with parameters  $\mu_{STOP}$  and  $\sigma_{STOP}$ . If  $x_{STOP}$  arrived at the threshold before  $x_{GO}$ , the trial was considered successfully stopped, and thus contributed to the inhibition function. This process was carried out for all  $t_d$  in each simulation with  $r_{STOP}$  chosen separately for each  $t_d$ ;  $\mu_{STOP}$  and  $\sigma_{STOP}$  were varied in order to minimize the difference between the simulated and experimentally obtained inhibition function. The resulting simulated inhibition functions were not significantly different from the observed ones (Fig. 11).

The estimates (in Hz) for  $\mu_{GO}$ ,  $\sigma_{GO}$ ,  $\mu_{STOP}$ , and  $\sigma_{STOP}$  are given in the first three columns of Table 4.

Finally, given these parameters the Hanes–Carpenter model allows us to predict the distribution of stop failure times for each stop signal delay. Fig. 12 shows the observed and predicted cumulative distribution functions for the four larger SSDs for each subject (for

<sup>7</sup> Note that this method of plotting chosen by Hanes and Carpenter tends to exaggerate deviations at the short and the long end of the distribution.

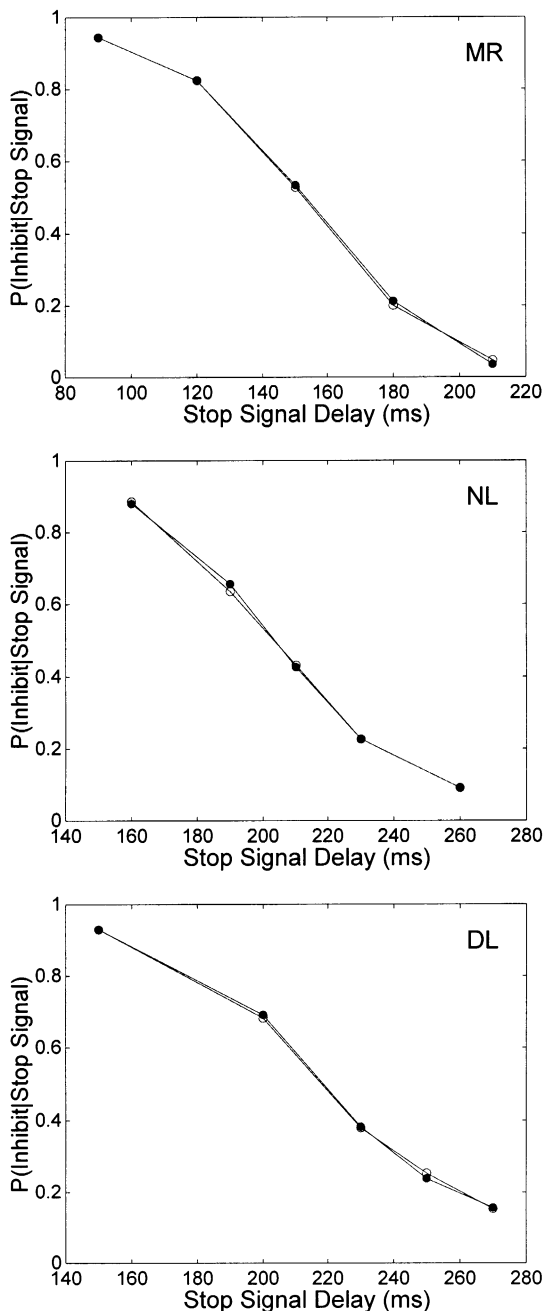


Fig. 11. Actual (filled symbols) and simulated (open symbols) inhibition functions. For the simulation method of parameter estimation  $\mu_{GO}$  and  $\sigma_{GO}$  are derived from these fits.

the shortest SSD there are not enough observations available).

For subjects DL and NL there were no significant differences between observed and estimated stop failure latency distributions for any stop signal delay. However, subject MR showed significant deviations from the model predictions for all four stop signal delays (Kolmogorov–Smirnov,  $P < 0.05$ ). Note that this difference between MR and the other subjects is in line with the results from testing the Logan–Cowan model.

### 5.2. Estimation from model equations

As shown in Appendix B, it is possible to derive explicit expressions for the latency distributions under the Hanes–Carpenter model. This is of interest in its own right, but it also allows estimation of the parameters without performing any simulations. In the first step of the procedure,  $\mu_{GO}$  and  $\sigma_{GO}$  were estimated by minimizing the sum-of-squares deviation between the observed frequencies in the control condition and the frequencies predicted from Eq. (B1) (bin size = 20 ms). In the second step,  $\mu_{STOP}$  and  $\sigma_{STOP}$  were estimated by minimizing the sum-of-squares deviation between the observed and the predicted frequencies in the stop failure conditions, using the observed inhibition frequencies as an estimate for the inhibition probabilities occurring in the predicted stop failure response times (c.f. Eq. (B2)). The parameter estimates obtained for  $\mu_{GO}$ ,  $\sigma_{GO}$ ,  $\mu_{STOP}$ , and  $\sigma_{STOP}$  are given in the three right columns in Table 4. Since they are very close to those found with the Monte Carlo simulations, the resulting model fits do not differ between the two methods applied here.

### 5.3. Discussion

The outcome of the test of the Hanes–Carpenter model is in accordance with our earlier results on the Logan–Cowan model. For subjects DL and NL both models yielded a satisfactory fit. This implies that the behavior of these two subjects can not only be described by a general race model mechanism, but their latency distributions in both the control and the stop failure condition do follow the specific parametric form imposed by the Hanes–Carpenter model. Moreover, the fact that the estimates of the stop signal processing time (SSPT) from the latter model are very close to the estimates derived from the Logan–Cowan model (c.f. Table 3) gives further credence to our conclusion that

Table 4

Estimated values of  $\mu_{GO}$ ,  $\sigma_{GO}$ ,  $\mu_{STOP}$ , and  $\sigma_{STOP}$  (in Hz) for all three subjects using the simulation method (left three columns) and the explicit formulation of the model (right three columns)

	Parameter estimates					
	From Monte Carlo simulations			From Hanes–Carpenter model equations		
	MR	NL	DL	MR	NL	DL
$\mu_{GO}$	5.12	5.00	4.88	5.11	4.96	4.86
$\sigma_{GO}$	0.66	0.84	0.90	0.66	0.90	1.06
$\mu_{STOP}$	12.3	30.4	48.2	12.3	30.4	48.2
$\sigma_{STOP}$	3.1	11.6	24.3	3.1	11.6	24.3

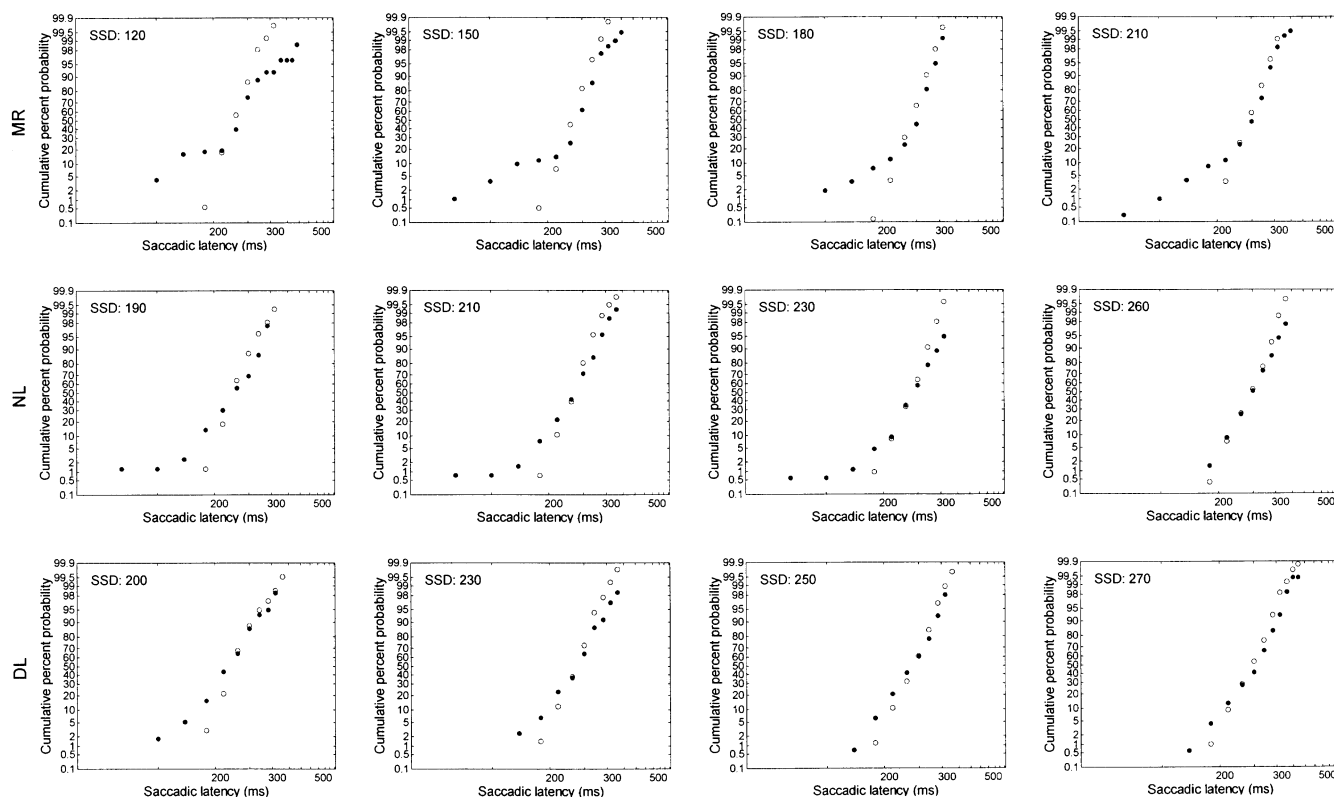


Fig. 12. Empirical latency distributions (filled symbols) and simulated distributions (open symbols) of stop failure trials for all subjects and the four higher SSDs. For the lowest SSD too few stop failure latencies were measured to permit a comparison between model and data on the basis of latency distributions. Data are shown as reciprobital plots. The parameters for the simulation are derived from the control condition and the inhibition functions. No further adaptation of parameters was made for the stop failure distributions.

auditory stop signals are more effective in inhibiting saccades towards visual targets (see above).

The situation is less transparent for subject MR. We found significant deviations from the Hanes–Carpenter model. This was to be expected given the violation of the lower bound of the distribution inequality by MR's data noted earlier: this violation ruled out any independent race model, including the Hanes–Carpenter version. MR's performance in the control trials did not differ much from the other two subjects. However, his stopping performance was about 50 ms slower, i.e. his inhibition function was shifted 50 ms to the left relative to the other subjects. The fact that MR was nearly 20 years older than the other two subjects may be an explanation for the slower stopping performance (c.f. Logan, 1994, p. 191.). Nonetheless, an examination of MR's hearing ability did not show any irregularities. In any event, a slower processing of the stop signal does not by itself explain the observed violation of the race model. Taking into account that the countermanding task gives the subject considerable leeway to carry out the stopping task, it is possible that certain strategic effects have contributed to the result. Note that MR is the only subject whose mean stop failure response time is not faster than the mean control latency suggesting

that this subject may have shifted his attention between the auditory and the visual modality. Such strategy effects would not be covered by the race model's independence assumptions.

## 6. General discussion

### 6.1. Summary

This paper reports an experiment where an auditory signal presented at different spatial positions served as a stop signal to inhibit saccades toward visual targets. Moreover, a new test of the race model was proposed and applied to the data. The three main experimental findings were: First, the effect of the auditory stop signal was similar to studies using a visual stop signal. In particular, the probability to inhibit a saccade reaches over the entire range from 1 to 0 depending on auditory stop signal delay, and average saccadic latency of stop failure responses was similar to that observed with visual stop signals. Second, we did not find an effect of spatial position of the stop signal relative to the go signal on stopping performance, i.e. a stop signal in close proximity to the target stimulus was neither

more nor less effective compared to a more distant stop signal. The third finding was the measurement of hypometric saccades and decreasing peak velocities in stop failure trials. This suggests an effect of the stop signal on the ongoing saccade dynamics that has not been observed in previous studies.

Using the established estimation techniques for the race model resulted in stop signal processing times of about 60 ms. Taking the faster peripheral processing time of auditory stimuli into account this estimate concurs with those found in related saccadic countermanding studies using visual stop signals. Moreover, the performance of two of the subjects were in good agreement with the predictions of the race model, while a third subject did not pass the distribution inequality test.

### 6.2. *Stop signal modality effects*

In this experiment, we employed auditory stop signals only, so no direct comparison with inhibitory performance under a visual stop signal is possible. Nonetheless, given that the stop failure latencies observed here were similar to those observed under visual stop signals (Hanes & Carpenter, 1999; Logan & Irwin, 2000), there is no indication in our data of a dramatic effect of stop signal modality on observable latencies beyond effects of stop signal intensity and differences in peripheral processing of the stop signal. This outcome was not obvious in the light of studies suggesting that — compared to a visual stimulus — an auditory signal may have a weaker effect on the fixation neurons in the superior colliculus (SC) (e.g. Taylor, Klein, & Munoz, 1999).

Moreover, the recent study by Cabel, Armstrong, Reingold, and Munoz (2000) performing a direct comparison of auditory, visual, and combined visual-auditory stop signals came to a different conclusion. A broad-band noise burst (auditory), a central fixation point (visual), and a combination of both were presented with equal probability on about one-third of the trials. Stop signal processing time estimates were longer for auditory stop signals (201 ms) than for signals with a foveal visual component (visual 113 ms, combined 91 ms). The authors attribute this difference in modality effectiveness to the role of saccade-related neurons in the intermediate layers of the superior colliculus. These neurons receive convergent auditory and visual inputs, but in experiments with awake monkeys (Frens & Van Opstal, 1996) the magnitude of the visual responses recorded from these neurons tended to be much greater than that of auditory responses. Consequently, a developing motor program will not immediately be affected by the auditory stop signal, but the auditory information must first be processed in higher centers before being relayed to the preoculomotor areas.

This interesting hypothesis suggested by Cabel et al. (2000) deserves further scrutiny. However, the difference between their results and those reported here may be explained in part by top-down mechanisms to halt the eye movement. These top-down mechanisms, explicitly mentioned by those authors, are influenced both by instruction (how important is it to obey the stop signal?) and by the a priori probability of a stop signal (of a specific modality) to occur (c.f. Logan, 1981). In the Cabel et al. experiment, the probability for a single auditory stop signal to occur in any given trial was only 12.5%. It is plausible, therefore, that subjects allocated most of their attention to the visual modality for efficient processing of the visual go and stop signals, and that the presentation of a stop signal in the unexpected auditory modality may have contributed to a slowdown of the stop signal processing (c.f. Spence & Driver, 1997). This hypothesis is supported by the shape of their inhibition functions for auditory stop signals: they were less steep than for visual or combined stop signals, and the probability to inhibit a response due to an auditory stop signal alone was 50% or less for four of the six subjects even when the stop signal was presented simultaneously with the go signal. In comparison, the inhibition functions obtained in our experiment were very similar in shape to those typically found with visual stop signals.

### 6.3. *Stop signal position effects*

An auditory stop signal in close proximity to the target stimulus was neither more nor less effective compared to a more distant stop signal. This negative result suggests that the inhibition mechanism either does not have access to, or does not make use of, the location information. From a functional point of view, this is consistent with the fact that successful inhibition only requires detection, but not localization of the stop signal. On the other hand, studies of visual-auditory interaction in the focused attention paradigm indicate that spatial distance of an irrelevant cue of one modality has a systematic effect on the detection of a target stimulus in the other modality: saccadic responses to the target stimulus are the faster the smaller the distance between the stimuli (Frens, Van Opstal, & Van der Willigen, 1995; Colonius & Arndt, 2001). The observation that the spatial position of the stop signal did not influence stopping behavior suggests, however, that the inhibitory processes take place at a level different from and, most likely, higher than the processes underlying the focused attention task. Our results are in line with the recent study by Asrress and Carpenter (2001) showing that central and peripheral visual stop signals did not differ with respect to their effect on SSPT. Presenting central and peripheral stop signals in the same trial appeared to shorten the SSPT to a degree

consistent with an independent probability summation mechanism. Thus, the authors conclude that information from different parts of the visual field is equally effective in countermanding, contrary to the suggestion by Schall and Thompson (1999).

These behavioral results are partly corroborated by neurophysiological studies showing that at least two different neural structures are involved in oculomotor control. Hanes et al. (1998) have shown that cells with movement- and fixation-related activity within the frontal eye field (FEF) generate signals sufficient to control eye movement, whereas orienting responses under bimodal stimulation have been related to activity patterns in the deep layers of the superior colliculus (SC) (e.g. Wallace, Meredith, & Stein, 1993; Meredith, 1999.). The FEF neurons have inhibitory connections to the SC, and lesions in this area result in disinhibition of saccades towards exogenous signals (Rafal & Henik, 1994). However, recent evidence shows that the SC may be involved in these inhibitory processes as well (Hanes & Paré, 1998). Both structures are organized in an equivalent topographical manner, and in particular neurons from the dorsal FEF associated with cognitive operations project on SC neurons with corresponding visual receptive and/or movement fields (Sommer & Wurtz, 2000). FEF afferents preferentially terminate on multisensory neurons in SC (Meredith, 1999) and FEF neurons with movement activity preceding saccades to visual targets are also active before saccades to auditory targets (Russo & Bruce, 1994; Schall, 1991). While movement cells show similar bursts for auditorily and for visually evoked saccades, visuomovement cells often show weaker responses to auditory targets (Russo & Bruce).

#### 6.4. Saccade trajectory effects

An interesting result of the experiment is the detection of hypometric amplitudes and decreasing peak velocities in stop failure trials. The amount of hypometry increased monotonically with temporal distance from the stop signal. While Hanes and Schall (1995) did not find such an effect in their data from the macaque, Kudo and Ohtsuki (1998) report hypometric amplitudes of a fast elbow extension in stop failure trials (for further evidence see also Gao & Zelaznik (1991)). The corresponding decrease of saccadic amplitudes and peak velocities indicates that the main sequence characteristics of the saccades are preserved under stop signal conditions. In any event, our finding suggests an effect of the stop signal on the ongoing saccade dynamics unfolding itself over time. Note, however, that this hypothesis is difficult to reconcile with the assumption of independence between STOP and GO processes of the race model.

#### 6.5. Status of the race model

The race model has been quite successful in describing performance on various stop signal tasks (Logan & Irwin, 2000). On the other hand, as pointed out in Logan (1994), it does not describe the nature of the processes that race against each other since it only depends on their finishing times. Nonetheless, hypotheses about the nature of the underlying processes are often expressed in terms of reaction times or of factors affecting it. Thus, the race model does put certain constraints on any process model within the general race framework. A case in point are the independence assumptions about the finishing times of the STOP and the GO processes. As pointed out above in the discussion of the test of the Logan–Cowan model, a satisfactory agreement between observed and predicted stop failure latencies is not sufficient as a test of the independence assumptions even though the overall estimate for the stop signal processing time may be quite accurate (Band, 1997). In this study, we found good agreement with the race model predictions for two of the subjects, while the third (MR) did not pass the distribution inequality test specified in Proposition 1. Note that a similar observation was made by Hanes and Carpenter (1999) for one subject (RC) exhibiting an elongated long-latency tail at shorter stop signal delays. They interpreted this finding as a slowing of the rate of rise of the GO process when the STOP process reaches its threshold, that is, as a violation of stochastic independence. Our observation of hypometric saccades and decreasing peak velocities in stop failure trials would certainly be in line with such an interpretation. Obviously, however, the data base is too sparse yet in order to conclude that the race model is in serious trouble.

The Hanes et al. (1998) study presents a very serious effort to probe the independence assumptions of the race model in a more direct way by recording from single cells in the FEFs of macaque monkeys during a stop task. Under the premise that the rise of the average discharge rates of fixation-related and movement-related FEF cells represent the STOP and the GO process activation, respectively, they were able to show that the activity of single FEF neurons is not different in non-cancelled and latency-matched control trials.<sup>8</sup> This suggests that at least at the level of the FEF, the GO process and the STOP process are context independent, i.e. that the distribution of the GO process is the same whether or not a stop signal is present. Note, however, that this important observation does not also confirm the assumption of stochastic independence

<sup>8</sup> For details of their procedure we must refer to Hanes et al. (1998).

between the two processes. A test of the latter assumption would require simultaneous recordings of the activity of a pair of fixation- and movement-related neurons so that their bivariate distribution function becomes available.<sup>9</sup>

**Acknowledgements**

This research was supported by a grant from Deutsche Forschungsgemeinschaft to H. Colonius (SFB 517/C3, Neurokognition). We thank the reviewers for their helpful suggestions.

**Appendix A. Proof of the Proposition**

The proof is based on the following lemma communicated by Erhard Cramer (Department of Mathematics, Oldenburg University):

**Lemma 1.** (Cramer). *Let  $X, Y$  be stochastically independent random variables with continuous distribution functions  $F_X, F_Y$ , respectively, such that  $F_X(0) = F_Y(0) = 0$  and  $P(X < Y) > 0$ . Then*

$$F_X(x) \leq P(X \leq x \mid X < Y)$$

for all  $x < 0$ .

**Proof 1.**

$$\begin{aligned} P(X \leq x, X < Y) &= \int_0^\infty P(X \leq x, X < t) dF_Y(t) \\ &= \int_0^x P(X \leq t) dF_Y(t) + \int_x^\infty P(X \leq x) dF_Y(t) \\ &= \int_0^x F_X(t) dF_Y(t) + F_X(x) \int_x^\infty dF_Y(t). \end{aligned}$$

On the other hand,

$$P(X < Y)F_X(x) = F_X(x) \int_0^\infty F_X(t) dF_Y(t). \tag{A4}$$

Thus, the claim of the lemma amounts to

$$\begin{aligned} &F_X(x) \int_0^\infty F_X(t) dF_Y(t) \\ &\leq \int_0^x F_X(t) dF_Y(t) + F_X(x) \int_x^\infty dF_Y(t), \end{aligned}$$

or

$$\begin{aligned} &F_X(x) \int_x^\infty F_X(t) dF_Y(t) - F_X(x) \int_x^\infty dF_Y(t) \\ &\leq -F_X(x) \int_0^x F_X(t) dF_Y(t) + \int_0^x F_X(t) dF_Y(t). \end{aligned}$$

Collecting terms,

$$\begin{aligned} &-F_X(x) \int_x^\infty [1 - F_X(t)] dF_Y(t) \\ &\leq [1 - F_X(x)] \int_0^x F_X(t) dF_Y(t). \tag{A1} \end{aligned}$$

Since the left side of Eq. (A1) is  $< 0$  and the right side is  $\geq 0$  it is valid for any  $x > 0$ . QED.

**Proof 2.** The lower bound of Eq. (5) follows directly from the lemma by replacing  $F_X$  by  $F_{GO}(t)$  and  $P(X \leq x \mid X < Y)$  by  $P[T_{GO} \leq t \mid T_{GO} < T_{STOP} + t_d]$ . For the upper bound,

$$\begin{aligned} F_{GO}(t) &= P[T_{GO} \leq t \mid \text{no stop signal presented}] \\ &= P[T_{GO} \leq t \mid T_{GO} < T_{STOP} + t_d] \\ &\quad P(T_{GO} < T_{STOP} + t_d) \\ &\quad + P[T_{GO} \leq t \mid T_{GO} > T_{STOP} + t_d] \\ &\quad P(T_{GO} > T_{STOP} + t_d) \\ &\geq P[T_{GO} \leq t \mid T_{GO} < T_{STOP} + t_d] \\ &\quad P(T_{GO} < T_{STOP} + t_d), \end{aligned}$$

where the equality in the first line follows from context independence. Dividing by  $P(T_{GO} < T_{STOP} + t_d)$  yields the upper bound of the proposition. QED.

**Appendix B. Hanes–Carpenter model**

The LATER model (Carpenter, 1981) assumes a linear rise  $r$  of the GO process  $t_{GO}$  to a fixed threshold  $\theta$  starting from an initial activity level  $s_0$ , i.e.

$$s_0 + r * t_{GO} = \theta.$$

Assuming  $r$  to be the realization of a normally distributed random variable  $R$  with mean  $\mu_{GO}$  and variance  $\sigma_{GO}^2$  and rearranging the above equation leads to an expression for the GO process random variable  $T_{GO}$ :

$$T_{GO} = (\theta - s_0) / R.$$

Since the distribution of  $R$  is given, the density of  $T_{GO}$  follows from a standard rule for the derivation of the density of a function of a random variable (c.f. Breiman, 1968):

$$f_{GO}(t) = \frac{\theta - s_0}{\sigma_{GO} \sqrt{2\pi t^2}} \exp \left[ - \left( \frac{\theta - s_0}{t} - \mu_{GO} \right)^2 / (2\sigma_{GO}^2) \right]. \tag{B1}$$

<sup>9</sup> Such recordings have been started (J. Schall, personal communication, June 2000).

In the Hanes–Carpenter model an analogous density is assumed for the STOP process with corresponding parameters  $\mu_{\text{STOP}}$  and  $\sigma_{\text{STOP}}$ . Under the independent race assumption this yields the following expression for the density of stop failures:

$$f_{\text{GO}}(t; t_d) = \frac{d}{dt} P[T_{\text{GO}} \leq t \cap T_{\text{GO}} < T_{\text{STOP}} + t_d] / (1 - q(t_d)) \\ = f_{\text{GO}}(t) \times [1 - F_{\text{STOP}}(t - t_d)] / (1 - q(t_d)). \quad (\text{B2})$$

## References

- Asrress, K.N., Carpenter, R.H.S. (2001). Saccadic countermanding: a comparison of central and peripheral stop signals. *Vision Research* (submitted).
- Band, G.P.H. (1997). Preparation, adjustment, and inhibition of responses. *Academisch Proefschrift*. Universiteit van Amsterdam.
- Breiman, L. (1968). *Probability*. Reading, MA: Addison-Wesley.
- Cabel, D. W. J., Armstrong, I. T., Reingold, E., & Munoz, D. P. (2000). Control of saccade initiation in a countermanding task using visual and auditory stop signals. *Experimental Brain Research*, *138*, 431–441.
- Carpenter, R. H. S. (1981). Oculomotor procrastination. In D. F. Fischer, R. A. Monty, & J. W. Senders, *Eye movements: cognition and visual perception* (pp. 237–246). Hillsdale: Erlbaum.
- Carpenter, R. H. S., & Williams, M. L. L. (1995). Neural computation of log likelihood in the control of saccadic eye movements. *Nature*, *377*, 59–62.
- Colonius, H. (1990). A note on the stop signal paradigm, or how to observe the unobservable. *Psychological Review*, *97*, 309–312.
- Colonius, H., & Arndt, P. A. (2001). A two stage-model for visual-auditory interaction in saccadic latencies. *Perception and Psychophysics*, *63*, 126–147.
- De Jong, R., Coles, M. G. H., Logan, G. D., & Gratton, G. (1990). In search of the point of no return: the control of response processes. *Journal of Experimental Psychology: Human Perception and Performance*, *16*, 164–182.
- Frens, M. A., & Van Opstal, A. J. (1996). Visual-auditory interactions modulate saccade-related activity in monkey superior colliculus. *Brain Research Bulletin*, *16*, 211–224.
- Frens, M. A., Van Opstal, A. J., & Van der Willigen, R. F. (1995). Spatial and temporal factors determine auditory–visual interactions in human saccadic eye movements. *Perception and Psychophysics*, *57*, 802–816.
- Gao, L., & Zelaznik, H. N. (1991). The modification of an already-programmed response: a new interpretation of Henry and Harrison (1961). *Journal of Motor Behavior*, *23*, 221–223.
- Hanes, D. P., & Carpenter, R. H. S. (1999). Countermanding saccades in humans. *Vision Research*, *39*, 2777–2791.
- Hanes, D. P., & Paré, M. (1998). Neural control of saccade production studied with the countermanding paradigm: superior colliculus. *Society for Neuroscience Abstracts*, *21*, 418.
- Hanes, D. P., & Schall, J. D. (1995). Countermanding saccades in macaque. *Visual Neuroscience*, *12*, 929–937.
- Hanes, D. P., & Schall, J. D. (1996). Neural control of voluntary movement initiation. *Science*, *271*, 427–430.
- Hanes, D. P., Patterson, W. F., & Schall, J. D. (1998). Role of frontal eye fields in countermanding saccades: visual, movement, and fixation activity. *Journal of Neurophysiology*, *79*, 817–834.
- Kudo, K., & Ohtsuki, T. (1998). Functional modification of agonist-antagonist electromyographic activity for rapid movement inhibition. *Experimental Brain Research*, *122*, 23–30.
- Lappin, J. S., & Eriksen, C. W. (1966). Use of a delayed signal to stop a visual reaction-time response. *Journal of Experimental Psychology*, *72*, 805–811.
- Leigh, R. J., & Zee, D. S. (1999). *The neurology of eye movements* (3rd edn). New York: Oxford University Press.
- Logan, G. D. (1981). Attention, automaticity, and the ability to stop a speeded choice response. In J. Long, & A. D. Baddeley, *Attention and performance IX* (pp. 205–222). Hillsdale, NJ: Erlbaum.
- Logan, G. D. (1994). On the ability to inhibit thought and action: a usersguide to the stop signal paradigm. In D. Dagenbach, & T. H. Carr, *Inhibitory processes in attention, memory and language* (pp. 189–239). San Diego, CA: Academic Press.
- Logan, G. D., & Cowan, W. B. (1984). On the ability to inhibit thought and action: a theory of an act of control. *Psychological Review*, *91*, 295–327.
- Logan, G. D., & Irwin, D. E. (2000). Don't look! Don't touch! Inhibitory control of eye and hand movements. *Psychonomic Bulletin and Review*, *7*, 107–112.
- Meredith, A. M. (1999). The frontal eye fields target multisensory neurons in cat superior colliculus. *Experimental Brain Research*, *128*, 460–470.
- Ollman, R. T. (1973). Simple reactions with random countermanding of the 'go'-signal. In S. Kornblum, *Attention and performance IV* (pp. 571–581). New York: Academic Press.
- Osman, A., Kornblum, S., & Meyer, D. (1986). The point of no return in choice reaction time: controlled and ballistic stages of response preparation. *Journal of Experimental Psychology: Human Perception and Performance*, *12*, 243–258.
- Rafal, R., Henik, A. (1994). *The neurology of inhibition: integrating controlled and automatic processes*. In: D. Dagenbach, T.H. Carr (Eds.). *Inhibitory processes in attention, memory, and language*. London: Academic Press, pp. 1–51.
- Russo, G. S., & Bruce, C. J. (1994). Frontal eye field activity preceding aurally guided saccades. *Journal of Neurophysiology*, *71*, 1250–1253.
- Schall, J. D. (1991). Neural activity related to visually guided saccades in the frontal eye fields of rhesus monkeys: comparison with supplementary eye fields. *Journal of Neurophysiology*, *66*, 559–579.
- Schall, J. D., & Thompson, K. G. (1999). Neural selection and control of visually guided eye movements. *Annual Review of Neuroscience*, *22*, 241–259.
- Sommer, M. A., & Wurtz, R. H. (2000). Composition and topographic organization of signals sent from the frontal eye field to the superior colliculus. *Journal of Neurophysiology*, *83*, 1979–2001.
- Spence, C., & Driver, J. (1997). On measuring selective attention to an expected sensory modality. *Perception and Psychophysics*, *59*, 389–403.
- Stein, B. E., & Meredith, A. M. (1993). *The merging of the senses*. Cambridge, MA: MIT Press.
- Taylor, T. L., Klein, R. M., & Munoz, D. P. (1999). Saccadic performance as a function of the presence and disappearance of auditory and visual fixation stimuli. *Journal of Cognitive Neuroscience*, *11*, 206–213.
- Wallace, M. T., Meredith, M. A., & Stein, B. E. (1993). Converging influences from visual, auditory, and somatosensory cortices onto output neurons of the superior colliculus. *Journal of Neurophysiology*, *69*, 1797–1809.